

## Numerical simulation of titanium alloy machining in electric discharge machining process

XIE Bao-cheng<sup>1,2</sup>, WANG Yu-kui<sup>1,2</sup>, WANG Zhen-long<sup>1,2</sup>, ZHAO Wang-sheng<sup>3</sup>

1. Key Laboratory of Micro-systems and Micro-structures Manufacturing of Ministry of Education, Harbin Institute of Technology, Harbin 150001, China;
2. School of Mechatronics Engineering, Harbin Institute of Technology, Harbin 150001, China;
3. School of Mechanical Engineering, Shanghai Jiao Tong University, Shanghai 200240, China

Received 10 May 2011; accepted 25 July 2011

**Abstract:** An axisymmetric three-dimensional thermo-physical model for the electrical discharge machining of titanium alloy was developed using finite element method. To efficiently predict the temperature distribution and the material removal rate, the model considers some realistic parameters such as the plasma channel radius based on discharge current and discharge duration, the latent heat of melting and evaporation, the percentage of discharge energy transferred to the workpiece and Gaussian distribution of heat flux. Numerical simulation of the single spark discharge of titanium alloy machining in electric discharge machining process was carried out using software ANSYS. The effect of various process parameters on temperature distributions along the radius of the workpiece was reported. Finally, the model was validated through EDM experiments, showing that it can efficiently predict material removal rate.

**Key words:** titanium alloy; electrical discharge machining; thermo-physical model; finite element method

### 1 Introduction

Titanium alloys are widely used in many industrial and commercial applications such as aerospace, chemical, automotive, medical and sporting goods industries and in many corrosive environments [1–4] because of titanium alloys' excellent properties such as a shock resistance, high specific strength, high temperature strength and exceptional corrosion resistance. However, titanium alloys are difficult to machine using the traditional machining techniques due to their high spring-back characteristics, high chemical reactivity and low heat-conduction coefficient, which leads to rapid tool wear during machining of titanium alloys, in turn increases the manufacturing cost [5–6].

The electrical discharge machining (EDM) process is the most popular among the non-conventional machining processes. The erosion process of EDM is that the discharge sparks in gap generate enough heat to melt and even vaporize some of the material on the surface of workpiece, so any difficult-to-cut material can be cut in

EDM as long as the material can conduct electricity. However, the complex nature of the process involves simultaneous interaction of thermal, mechanical, chemical and electrical phenomena, which makes process model very difficult. Thus, many researchers have focused their attention on the titanium alloy machining in EDM process by experiments; however, few theoretical analysis of the erosion mechanism of titanium alloy in EDM process was involved [7–9].

In this work, an attempt has been made to study the erosion mechanisms of titanium alloy in EDM process through temperature distribution. According to the important factors of the EDM process such as conduction, convection, thermal properties of material with temperature, the latent heat of melting and evaporation, the percentage of discharge energy transferred to the workpiece, the thermal property of titanium alloy, the plasma channel radius and Gaussian distribution of heat flux based on discharge duration, ANSYS version 12.0 has been used to develop and calculate a numerical model of the EDM process.

## 2 Thermal model of EDM process

The EDM process can be described as the thermal process, as shown in Fig. 1. Material is heated up by the action of high energy electrical sparks. The spark melts and vaporizes a small area on the electrode surface. At the end of the pulse on-time, a small amount of molten material is ejected from the surface, producing craters on the workpiece surface. The EDM process involves simultaneous interaction of thermal, mechanical, chemical and electromagnetism phenomena, which makes process model very difficult, so the following assumptions are made to simplify the model.

1) The model is developed for a single spark; 2) Heat transfer is mainly by conduction and convection. Radiation heat losses are neglected; 3) The material over the melting point is removed completely after the end of spark discharge; 4) EDM spark channel is considered a uniform cylindrical column; 5) Work piece materials are homogeneous and isotropic in nature, and thermal properties of the material are temperature dependent for temperatures below 800 °C, they are kept constant when temperatures are over this value.

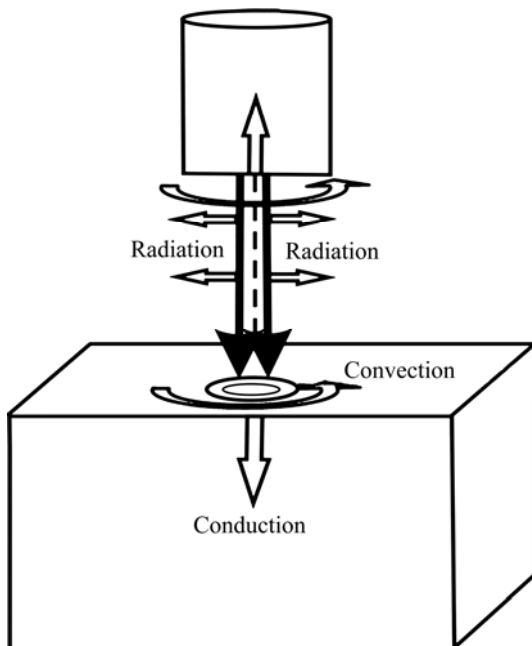


Fig. 1 Thermal model of EDM process

### 2.1 Governing equation and boundary conditions

The governing partial differential equation considering boundary conditions for the temperature distribution in a cylindrical coordinate system is

$$\frac{1}{\partial} \frac{\partial T}{\partial t} = \frac{\partial^2 T}{\partial^2 r} + \frac{1}{r} \frac{\partial T}{\partial r} + \frac{\partial^2 T}{\partial^2 z} \quad (1)$$

where  $r$  and  $z$  are the coordinates of cylindrical work

domain;  $T$  is temperature;  $\alpha$  is the thermal diffusivity of the material which can be written as  $\alpha=k/(\rho c_p)$ ,  $\rho$  is the average material density,  $c_p$  is the average specific heat capacity, and  $k$  is the thermal conductivity.

The associated initial and boundary conditions for governing partial differential equation are

$$\text{Initial condition : } t = 0, T = T_0$$

$$\text{Boundary condition : } t > 0, -k \frac{\partial \theta}{\partial z} = q(t), 0 \leq r \leq R(t);$$

$$-k \frac{\partial \theta}{\partial z} = 0, R(t) \leq r$$

$$\text{Convection : } -k \frac{\partial T}{\partial z} \Big|_r = h(T - T_f) \Big|_r$$

### 2.2 Plasma channel radius

The plasma channel radius, the size of heat flux on the workpiece surface, is an important factor in the model of the EDM process. The shape and evolution of the plasma channel radius have been studied by many authors. In practice, it is extremely difficult to experimentally measure spark radius due to a very short pulse duration of the order of few microseconds. Some researchers considered the plasma channel radius is time dependent, others considered the plasma channel radius is time and current dependent. IKAI and HASHIGUCHI [10] derived a semi-empirical equation of spark radius termed as “equivalent heat input radius” which is assumed as a function of the duration of the spark,  $t(\mu\text{s})$ , and the current,  $I(\text{A})$ . It is more realistic compared with the other approaches.

$$R(t) = 0.00204 I^{0.43} t^{0.44} \quad (2)$$

### 2.3 Heat input to workpiece

It has been reported that the isothermal curves obtained for EDM thermal model can be approximated by Gaussian distribution. YADAV et al [11] reported a heat flux equation for EDM considering the Gaussian distribution. To simply the simulation, since the Gaussian curve does not mathematically become zero until infinity, it is necessary to select some finite large value of its argument to represent the bottom of the crater. Usually six-times of  $\sigma(-3\sigma, +3\sigma)$  is taken for dropping the response to 0.25% of its initial value, i.e., 99.75% of the value between  $r=\mu-3\sigma$  and  $r=\mu+3\sigma$ . The profile of a three-dimensional crater can be obtained by rotating the Gaussian curve around the vertical axis [12].

$$q(r) = \frac{4.57\eta UI}{\pi R(r)^2} \exp\left(-\frac{4.5r^2}{R(t)^2}\right) \quad (3)$$

where  $\eta$  is the percentage of discharge energy transferred to the workpiece;  $U$  is the discharge voltage;  $I$  is the

discharge current. Energy distribution ( $\eta$ ) is an important factor in this equation as it governs the fraction of energy lost to cathode. DIBITONTO et al [13] predicted that about 8% of the total heat supplied is absorbed by anode and about 18% is absorbed by cathode. SHANKAR et al [14] calculated that 40%–45% of the heat input is absorbed by the workpiece. XIA et al [15] discovered that the energy distribution to anode and cathode is about 40% and 25%, respectively. In this simulation, the value of  $\eta$  of 0.3 has been chosen to estimate its effect on the MRR.

#### 2.4 Latent heat of melting and evaporation

The temperature of the plasma channel was in the range of 8 000–10 000 K and decreased slowly with time in EDM process, and workpiece was heated above the melting point. The phase change process required an energy input in order to keep temperature constant. Thus, the effect of latent heat was considered to make the model more realistic. Therefore, phase change was dealt with in the form of enthalpy instead of specific heat capacity of material. The quantity of energy change was equal to the quantity of enthalpy change.

The energy required to melt and vaporize the cathode material per unit volume can be estimated, as given in Eq. (4):

$$H_m = \int_{T_0}^{T_m} \rho c_p(t) dt + \rho L_m \quad (4)$$

$$H_v = \int_{T_0}^{T_m} \rho c_p(t) dt + \rho L_m + \int_{T_m}^{T_b} \rho c_p(t) dt + \rho L_v$$

where  $c_p(t)$  is specific heat capacity of workpiece;  $L_m$  and  $L_v$  are the latent heat of melting and evaporation respectively;  $H_m$  and  $H_v$  are the total absorbed heat of melting and evaporation.

#### 2.5 Material flushing efficient

In the EDM, a small amount of molten material is ejected from the surface at the end of the pulse duration. JILANLI et al [16] found that, if the assumption is used that all of the molten material is effectively ejected, the values of material removal rates predicted are higher than the experimentally measured ones. DIBITONTO et al [13] found that material flushing coefficient increases with the increase of the current and discharge duration. PEREZ et al [17] found that for a certain EDM regime, the crater represents about 35% of the total molten volume. Thus, a proper material flushing coefficient of the material removal becomes critical. The material flushing coefficient value is 15%.

#### 2.6 Thermo-physical properties of Ti–6Al–4V

The thermo-physical properties of Ti–6Al–4V are as follows [18]: density,  $\rho=4\,500\text{ kg/m}^3$ ; specific heat

capacity,  $c_p(t)=505\text{--}624\text{ J/(kg}\cdot\text{°C)}$  in the range of 300–800 °C; thermal conductivity,  $k=7.4\text{--}16.5\text{ W/(m}\cdot\text{°C)}$  in the range of 300–800 °C; ambient temperature,  $T_0=25\text{ °C}$ ; melting point temperature,  $T_m=1\,660\text{ °C}$ ; boiling or vaporization temperature,  $T_b=3\,260\text{ °C}$ ; latent heat of fusion or melting,  $L_m=392\text{ kJ/kg}$ ; latent heat of vaporization,  $L_v=8\,750\text{ kJ/kg}$ .

#### 2.7 Solution of thermal model

The model of the EDM process was carried out using ANSYS software. A quarter of axisymmetric three-dimensional model was created with a dimension of  $60\text{ }\mu\text{m} \times 60\text{ }\mu\text{m} \times 60\text{ }\mu\text{m}$ . A non-uniformly distributed finite element mesh with elements mapped towards the heat-affected regions was meshed, with a total number of up to 32 000 elements (Fig. 2).

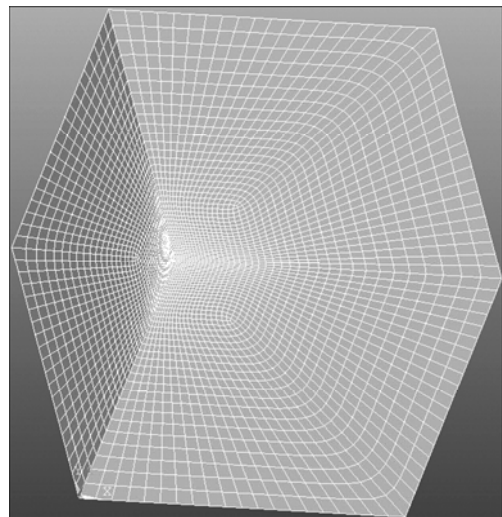


Fig. 2 Three-dimensional meshed model

The governing equation with boundary conditions mentioned above is solved by finite element method to predict the temperature distribution with the heat flux at the spark location and the discharge duration as the total time step. Figure 3 shows typical temperature contour for work material titanium alloy (Ti–6Al–4V) under machining conditions: current 0.84 A, and discharge duration 100  $\mu\text{s}$ .

### 3 Parametric analysis of thermal model

#### 3.1 Effect of current and pulse duration

The curve of the temperature distribution along radius of the center of discharge spot has been depicted for different values of current (0.11, 0.21, 0.42 and 0.84 A) and pulse duration (10, 20, 50 and 100  $\mu\text{s}$ ), as shown in Fig. 4. From Fig. 4, it is shown that the heat affected area goes on increasing with increase in current and pulse duration, while the maximal temperature does not

have the same trend. The reason is that the heat flux goes on decreasing with increase in current and pulse duration due to the plasma channel expanding. The larger the current and pulse duration are, the greater the plasma channel radius is. The larger the plasma channel radius is, the greater the area heated is.

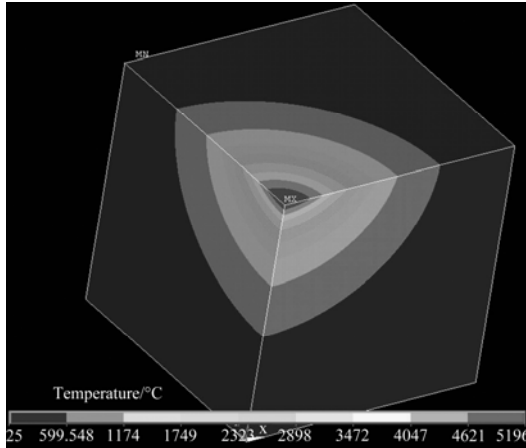


Fig. 3 Contour of temperature distribution at end of spark

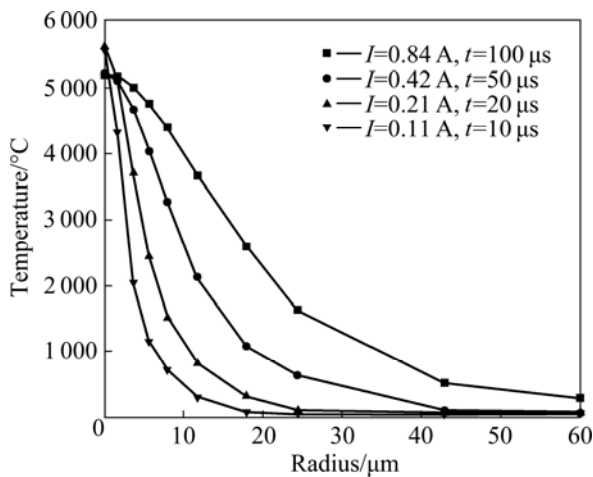


Fig. 4 Effect of current and pulse duration on temperature distribution

### 3.2 Heat input to workpiece

In Fig. 5, the temperature distribution along radial of the center of discharge spot is depicted, with different values of heat input to workpiece by adjusting the percentage of discharge energy. From Fig. 5, it is shown that the temperature at the center of discharge spot goes on increasing with increase in the percentage of discharge energy transferred to the workpiece. This is because the larger the percentage of energy is, the greater the heat transferred to the workpiece is.

### 3.3 Latent heat of melting and evaporation

In Fig. 6, temperature distribution along radius of the discharge spot was depicted with/without considering

the latent heat of melting and evaporation. From Fig. 6, it is shown that the temperature considering the latent heat of melting and evaporation is lower than that without considering the latent heat of melting and evaporation. The reason is that the phase change needs additional heat energy to change from solid to liquid and from liquid to gas in despite of the temperature keeping constant.

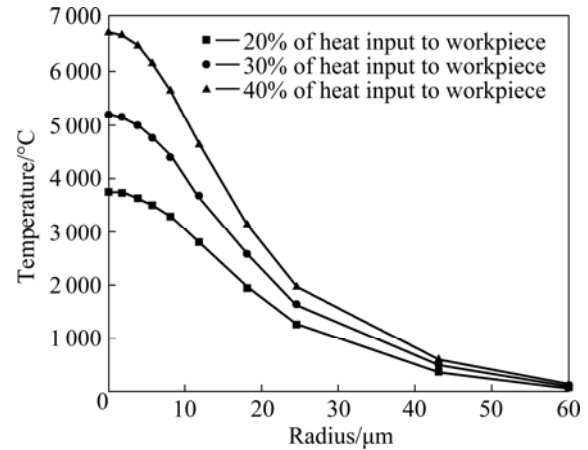


Fig. 5 Effect of percentage of energy on temperature distribution

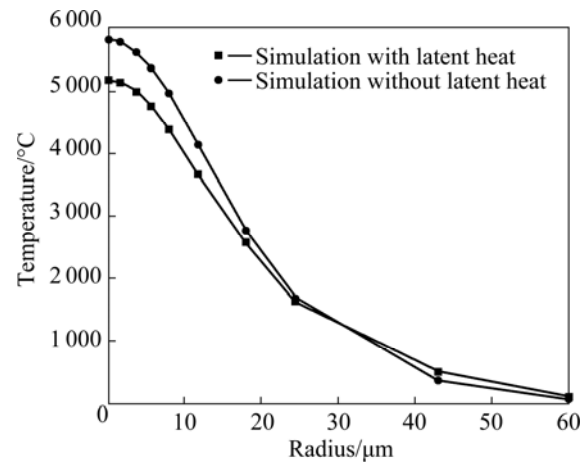


Fig. 6 Effect of phase change on temperature distribution

## 4 Experiment

The experiment conditions are as follows: equipment, multi-axis micro-EDM machine tool; electrode, red copper electrode; workpieces, Ti-6Al-4V plates of 1 mm-thick; working fluid, special EDM kerosene; polarity, negative polarity; servo voltage, 150 V. Figure 7 shows the SEM image of a hole machined under the following machine settings: current 0.84 A and discharge duration 100  $\mu$ s.

Aiming to experiment conditions, the corresponding numerical simulation was carried out to prove the reliability of the model through MRR both theoretically and experimentally.

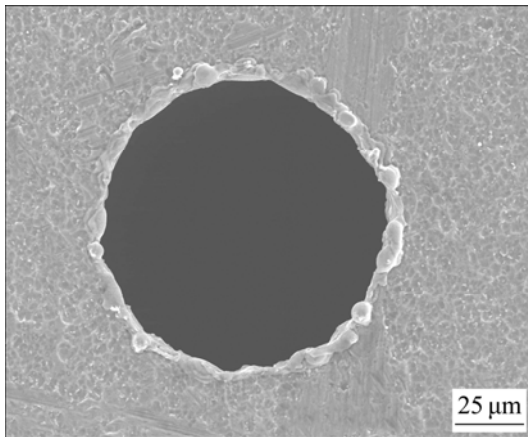


Fig. 7 SEM image of hole

From Table 1, the value of simulated MRR is higher than the experimental one. The main reason is that the value of simulated MRR is simply calculated by a volume of the single discharge using total machining time, considering the molten material ejected from the surface at the end of the pulse duration, and without considering the complex interaction of different physical phenomena.

Table 1 Comparison of predicted results

Current/ A	Pulse on- time/ $\mu$ s	Pulse off- time/ $\mu$ s	MRR/( $\text{mm}^3 \cdot \text{min}^{-1}$ )	
			Experiment	Simulation
0.11	10	5	0.066	0.062
0.21	20	20	0.109	0.120
0.42	50	5	0.509	0.380
0.84	100	20	1.19	0.95

## 5 Conclusions

1) An axisymmetric three-dimensional thermal model for the titanium alloy machining was developed using finite element method. Numerical analysis of the single spark discharge in electric discharge machining titanium alloy process was simulated by ANSYS version 12.0.

2) Some realistic parameters such as the latent heat of melting and evaporation, spark radius equation based on discharge current and discharge duration, the plasma channel radius and Gaussian distribution of heat flux, the percentage of discharge energy transferred to the workpiece have made our model closer to actual process conditions.

3) It was found that the MRR value predicted by our model is closer to the experimental result, indicating a worthwhile theoretical foundation for mechanism of material removal in EDM machining.

## References

- [1] GAO Hong-ming, BAI Yan, YANG Tian-dong. Double-sided gas tungsten arc welding process on TC4 titanium alloy [J]. Transactions of Nonferrous Metals Society of China, 2005, 15(5): 1081–1084.
- [2] SUN Zhong-gang, HOU Hong-liang, LI Hong. Effect of hydrogen treatment on microstructure and room temperature deforming properties of TC4 alloy [J]. The Chinese Journal of Nonferrous Metals, 2008, 18(5): 789–793. (in Chinese)
- [3] SONG Hui, WANG Zhong-jin, GAO Tie-jun. Effect of high density electropulsing treatment on formability of TC<sub>4</sub> titanium alloy sheet [J]. Transactions of Nonferrous Metals Society of China, 2007, 17(1): 87–92.
- [4] LI Mao-sheng, CHI Guan-xin, WANG Zhen-long. Micro electrical discharge machining of small hole in TC4 alloy [J]. Transactions of Nonferrous Metals Society of China, 2009, 19(s): s434–s439.
- [5] AHMET H, ULAS C. Electrical discharge machining of titanium alloy (Ti–6Al–4V) [J]. Applied Surface Science, 2007, 253: 9007–9016.
- [6] CHURI N J, PEI Z J, TREADWELL C. Rotary ultrasonic machining of titanium alloy (Ti–6Al–4V): Effects of tool variables [J]. Int J Precision Technology, 2007, 1(1): 85–96.
- [7] PETER F, WANG Zhi-gang, KAZUO Y, YUJI A. A fundamental study on Ti-6Al-4V's thermal and electrical properties and their relation to EDM productivity [J]. Journal of Materials Processing Technology, 2008, 202: 583–589.
- [8] YAN C L, YAN B H, CHANG Y S. Machining characteristics of titanium alloy (Ti–6Al–4V) using a combination process of EDM with USM [J]. Journal of Materials Processing Technology, 2009, 104: 171–177.
- [9] KAO J Y, TSAO C C, WANG S S, HSU C Y. Optimization of the EDM parameters on machining Ti–6Al–4V with multiple quality characteristics [J]. Int J Adv Manuf Technol, 2010, 47: 395–402.
- [10] IKAI T, HASHIGUSHI K. Heat input for crater formation in EDM [C]// Proceedings of International Symposium for Electro-machining, ISEM XI. Lausanne, Switzerland: EPFL, 1995: 163–170.
- [11] YADAV V, JAIN V K, DIXIT P M. Thermal stresses due to electrical discharge machining [J]. International Journal of Machine Tools and Manufacturing, 2002, 42: 877–888.
- [12] KANSAL H K. Numerical simulation of powder mixed electric discharge machining (PMEDM) using finite element method [J]. Mathematical and Computer Modeling, 2008, 42: 1217–1237.
- [13] DIBITONTO D D, EUBANK P T, PATEL M R, BARRUFET M A. Theoretical models of the electrical discharge machining process. I. A simple cathode erosion model [J]. Journal of Applied Physics, 1989, 66(9): 4095–4103.
- [14] SHANKAR P, JAIN V K, SUNDARAJAN T. Analysis of spark profiles during EDM process [J]. Machining Science Technology, 1997: 195–217.
- [15] XIA H, NISHIWAKI K, KUNIEDA M, NISHIWAKI N. Measurement of energy distribution in continuous EDM process [J]. J of JSPE, 1996, 62(8): 1141–1145. (in Japanese).
- [16] JILANI S T, PANDEY P C. Analysis and modeling of EDM [J]. Precise Engineering, 1982, 4(4): 215–218.
- [17] PEREZ R, CARRON J, RAPPAZ M, WALDER G, REVAZ B, FLUKIGER R. Measurement and metal lurgical modeling of the thermal impact of EDM discharges on steel [C]// Proceedings of the 15th International Symposium on Electromachining. Pennsylvania, USA: CIRP, 2007: 17–22.
- [18] ZHANG W J, REDDY B V, DEEVI S C. Physical properties of TiAl-base alloys [J]. Scripta Materialia, 2001, 45: 645–651.

## 电火花钛合金加工的数值模拟

解宝成<sup>1,2</sup>, 王玉魁<sup>1,2</sup>, 王振龙<sup>1,2</sup>, 赵万生<sup>3</sup>

1. 哈尔滨工业大学 微系统微结构制造教育部重点实验室, 哈尔滨 150001;
2. 哈尔滨工业大学 机电工程学院, 哈尔滨 150001;
3. 上海交通大学 机械与动力工程学院, 上海 200240

**摘 要:** 建立电火花钛合金加工的三维有限元轴对称热物理模型。为了更好地预测温度场分布和材料去除效率, 采用模型分析了基于电流和脉宽变化的等离子体半径、熔化和气化潜热、能量分配系数和高斯分布的热流密度等影响因素, 模拟了单脉冲电火花放电加工钛合金的温度场, 并研究了沿放电凹坑的半径方向上温度场分布的放电参数。通过实验数据的对比, 验证该模型在材料去除效率方面具有很好的预测效果。

**关键词:** 钛合金; 电火花加工; 热物理模型; 有限元方法

(Edited by YANG Hua)